Applied Radiation and Isotopes 128 (2017) 22–27

Contents lists available at ScienceDirect

Applied Radiation and Isotopes

journal homepage: www.elsevier.com/locate/apradiso

Scintigraphic imaging of *Staphylococcus aureus* infection using ^{99m}Tc radiolabeled aptamers

Sara Roberta dos Santos[a], Camila Maria de Sousa Lacerda[a], Iêda Mendes Ferreira[a], André Luís Branco de Barros[b], Simone Odília Fernandes[b], Valbert Nascimento Cardoso[b], Antero Silva Ribeiro de Andrade[a,*]

[a] Centro de Desenvolvimento da Tecnologia Nuclear (CDTN), Rua Professor Mário Werneck S/No, Cidade Universitária-Campus da UFMG, 31120-970 Belo Horizonte, MG, Brazil

[b] Departamento de Análises Clínicas e Toxicológicas - Faculdade de Farmácia, Universidade Federal de Minas Gerais (UFMG), Cidade Universitária – Campus da UFMG, 31270-091 Belo Horizonte, MG, Brazil

HIGHLIGHTS

- ^{99m}Tc radiolabeled *S. aureus* aptamers were evaluated for infection imaging.
- Identification of *S. aureus* infected areas was possible by scintigraphic images.
- High target to non-target ratios were obtained using the ^{99m}Tc radiolabeled aptamers.

ARTICLE INFO

Keywords:
Aptamer
Technetium-99m
Radiopharmaceutical
Bacterial infection
Diagnosis

ABSTRACT

Staphylococcus aureus is a specie of great medical importance associated with many infections as bacteremia and infective endocarditis as well as osteoarticular, skin and soft tissue, pleuropulmonary, and device related infections. Early identification of infectious foci is crucial for successful treatment. Scintigraphy could contribute to this purpose since specific radiotracers were available. Aptamers due to their high specificity have great potential for radiopharmaceuticals development. In the present study scintigraphic images of *S. aureus* infectious foci were obtained using specific *S. aureus* aptamers radiolabeled with ^{99m}Tc.

1. Introduction

Nuclear medicine could contribute to an accurate diagnosis of bacterial infections, since specific radiopharmaceuticals were developed. Infection specific radiopharmaceuticals can be used for diagnosis, decision-making in therapy and follow-up treatments. A variety of radiopharmaceuticals is used to detect infection, but long-term clinical use has shown that these probes cannot distinguish between infection and inflammation mainly because they are not specific to the target bacteria (Ferro-Flores et al., 2012).

The plethora of biological targeting molecules of radiopharmaceuticals ranges from antibodies, antibodies fragments, proteins, peptides and nucleic acid (Aerts et al., 2014). Nucleic acid aptamers are RNA or DNA oligonucleotides able of binding to a target molecule with high affinity and selectivity. The term “aptamers" derives from the Latin word "aptus," meaning “to fit” and the Greek word “meros”, meaning “part or region”. Nucleic acid aptamers are selected by an in vitro selection process termed SELEX (Systematic Evolution of Ligands by EXponential enrichment) through repeated rounds of partitioning and amplification from large random synthetic oligonucleotide library (Tuerk and Gold, 1990). They have been selected to a variety of target molecules such as proteins, peptides, amino acids, nucleotides, drugs, vitamins, organic and inorganic compounds, and whole cells (You et al., 2003).

Aptamers has advantages to other biomolecules as radiopharmaceuticals. Aptamers can be easily produced by in vitro conditions with high reproducibility and free of contaminants. They seem to be non-toxic and non-immunogenic, have small size (10–20 kDa) and fast clearance. The chemical synthesis allows alterations to become them more nuclease-resistant with modification at the 3' and 5' ends or by using modified nucleotides (Missailidis and Perkins, 2007). Lyophilized aptamers can be stored for years and, once reconstituted; they

* Corresponding author.
E-mail addresses: sararoberta7@hotmail.com (S.R.d. Santos), cmslacerda@gmail.com (C.M. de Sousa Lacerda), imendesf@yahoo.com.br (I.M. Ferreira), brancodebarros@yahoo.com.br (A.L.B. de Barros), simone@farmacia.ufmg.br (S.O. Fernandes), valbertncardoso@gmail.com (V.N. Cardoso), antero@cdtn.br (A.S.R. de Andrade).

http://dx.doi.org/10.1016/j.apradiso.2017.06.043
Received 23 March 2017; Received in revised form 9 May 2017; Accepted 27 June 2017
Available online 28 June 2017
0969-8043/ © 2017 Elsevier Ltd. All rights reserved.

can be boiled or subjected to many freeze-thaw cycles (Evtugyn et al., 2014). Besides, they were able to discriminate between closely related molecules, such as the presence or absence of a methyl group or hydroxyl group, or the ability to distinguish between D and L amino acids (Geiger et al., 1996). Due to the high specificity, large variety of potential targets, and the possibility of labeling with different radionuclides, aptamers have great potential for radiopharmaceuticals development. Since their discovery, several aptamers have been used as targeting molecule of radiopharmaceuticals in preclinical studies (Gijs et al., 2016).

Staphylococcus aureus is both a commensal bacterium and a human pathogen that may cause bacteremia and infective endocarditis as well as osteoarticular, skin and soft tissue, pleuropulmonary, and device related infections. This bacterium is the most common agent in skin and soft tissue infections, often being isolated from infected surgical wounds that can be foci for systemic infections. The early identification of infectious foci is critical to successful treatment of *S. aureus* infections (Robert and Chambers, 2005). In this study aptamers specific to *S. aureus* were radiolabeled with ^{99m}Tc and evaluated by scintigraphic imaging of bacterial infection-bearing mice.

2. Material and methods

2.1. Chemicals

The aptamers SA20, SA23 and SA34 (Cao et al., 2009) were synthesized by Integrated DNA Technologies (IDT) with the flowing modifications: an amino group linked to a 6 carbons spacer at the 3'end and an inverted thymidine at the 5' end. The ^{99m}Tc was obtained from a molybdenum generator (IPEN- São Paulo/Brazil). All other chemicals and reagents used were of analytical grade.

2.2. Microorganisms

Staphylococcus aureus (ATCC 25923) cells were cultured on BHI solid (Himedia Laboratories Pvt Ltd.) in petri dishes at 37 °C and subcultured every seven days.

2.3. Animals

Swiss mice were kept in cages with wood shavings, water and common food in ordinary shelves. All protocols were approved by the local Ethics Committee for Animal Experimentation of the Federal University of Minas Gerais (CEUA/UFMG), Protocol no. 108/2014.

2.4. Aptamers radiolabeling with ^{99m}Tc and radiochemical purity determination

Labeling with ^{99m}Tc was performed by the direct method (Correa et al., 2014). For the labeling reaction 111.6 μmol of tricine and 28.3 μmol of EDDA were added to 300 μL of 0.9% saline. Then, 10 μL of a mixture of aptamers SA20, SA23 and SA34 (200 pmol/μL each) followed by 100 μL of $SnCl_2{\cdot}2H_2O$ (8.9 mM in HCl 0.25 N) were added. The pH was adjusted to 7.0 with NaOH 1N. The bottle was sealed and vacuum was performed. The activity of 481 MBq of a ^{99m}Tc-pertechnetate solution ($Na^{99m}TcO_4$) was added. The solution was boiled in water bath for 15 min and then cooled. An oligonucleotide DNA library (random sequences) was labeled in the same way and used as control.

The radiochemical purity (RP) of ^{99m}Tc-aptamer complex was assessed by ascending instant thin-layer chromatography (TLC) using silica gel-coated fiber glass sheets and two solvent systems: (1) 100% acetone to determine the percentage of TcO_4^- and (2) NaCl 0.9% (w/v) solution with 5% NH_4OH to determine the percentage of TcO_2. The labeled product (^{99m}Tc-aptamer) remained at the point of application when 100% acetone was used as the mobile phase (Rf = 0) and the labeled product moved with the solvent front when NaCl 0.9% (w/v) solution with 5% NH_4OH was used as the mobile phase (Rf = 1). The RP was determined according to the following equation:

$$\textit{Radiolabeling yield}\ (\%) = 100 - (\%\ TcO_4^- + \%\ TcO_2)$$

2.5. Determination of radiolabeled aptamers binding to plasma proteins

A blood sample (6 mL) was collected from Swiss mice and the plasma fraction was separated by centrifugation (700*g*). EDTA (0.1 M) was used as anticoagulant. Aliquots (triplicate) of 50 μL of plasma were incubated with 45 μL of ^{99m}Tc-aptamers, at 37 °C, for 1 h and 3 h. After that, 1.5 mL of acetonitrile was added in each tube. The soluble and insoluble plasma fractions were separated by centrifugation (700*g*) and the radioactivity in the fractions was measured in a gamma counter (Wallac Wizard 1470-020 Gamma Counter, PerkinElmer Inc., Waltham, EUA). The percentage of radioactivity in the insoluble plasma fraction was determined by dividing the count in the insoluble plasma fraction by the total count (soluble fraction + insoluble fraction) and multiplying this value by 100.

2.6. Blood clearance

The ^{99m}Tc-aptamers (3.0 MBq) were administrated in Swiss mice (n = 7) through the tail vein. A small incision was made in the distal tail to enable rapid and reliable blood collection. Blood samples (20 μL) were collected at 5, 10, 15, 30, 60, 90, 120, and 240 min after administration. The samples were weighted and the radioactivity was measured in gamma counter. The percentage of injected activity per gram (%ID/g) and the mean ± SD in each sample were determined. The data were plotted as a function of time and blood clearance analysis was performed using GraphPad PRISM version 5.01 software. The distribution half-life and elimination half-life were calculated using non-linear regression.

2.7. Biodistribution studies

Three groups of Swiss mice (20–25 g) (n = 7) were used. The group 1 included animals infected with *S. aureus* that were inoculated with the ^{99m}Tc-aptamers. The group 2 comprised animals infected with *S. aureus* that were inoculated with a ^{99m}Tc-radiolabeled library (control). The group 3 consisted of healthy non-infected mice (which received 100 μL of saline in the right thigh) inoculated with the ^{99m}Tc-aptamers. The animals were anesthetized with a mixture of xylazine (15 mg/kg) and ketamine (80 mg/kg). The group 1 and group 2 were infected intramuscularly in the right thigh with 1 x 10^6 cells of *S. aureus* suspended in 100 μL of saline. A visible swelling was observed on infected thigh of all animals 24 h after the intervention.

Twenty-four hour after infection foci induction, 100 μL (35.9 MBq) of ^{99m}Tc-aptamers solution were injected by the tail vein of each animal of groups 1 and 3. The group 2 mice were submitted to the same procedure using the ^{99m}Tc-library. The groups 2 and 3 were used as controls.

The mice were euthanized at 3 h after the injection and tissue samples (blood, liver, spleen, stomach, heart, lung, kidneys, right thigh infected muscle and left thigh muscle) were dissected, weighed and their activities measured in a gamma counter. The results were expressed as the percentage of injected dose per gram of tissue (%ID/g). Target/non-target ratios were obtained from the analysis of radiation measured in the infected muscle of the right thigh in relation to radiation measured in the muscle of the left thigh.

2.8. Scintigraphic imaging

The animals were anesthetized by intraperitonial injection, as above mentioned, and placed in the prone position on a γ-camera equipped with a low-energy collimator (Nuclide TH 22, Mediso, Hungary). Five

minutes static planar images were acquired using a 256 × 256-pixel matrix. The images were acquired at 1 h and 3 h post-injection. The scintigrams were analyzed in the automatic regions of interest (ROI) draw around the infected right tight which were copied to the contralateral non-infected left tight. The ratios of the count in the target ROI to non-target ROI were calculated using the total counts.

2.9. Statistical analysis

All data are expressed as mean ± SD and they were analyzed by GraphPad PRISM version 5.01 software. The analysis of variance (ANOVA) with a confidence interval of 95% and Tukey multiple comparison test were used. A P value < 0.05 was considered to indicate a statistically significant difference.

3. Results and discussion

3.1. Determination of radiolabeled aptamers binding to plasma proteins

Swiss mice plasma was incubated with the ^{99m}Tc-aptamers and the plasma proteins fraction was precipitated in the presence of acetonitrile. The average binding of ^{99m}Tc-aptamers to plasma proteins (insoluble fraction) was 41.3 ± 3.0% at 1 h and 41.0 ± 0.5% at 3 h. The assay demonstrated that the aptamers are prone to non-specific binding to plasma proteins. This behavior can be explained in view of the negative aptamers charge and the presence of high amounts of positive charged amino acids in the plasma proteins (Henry et al., 2012).

3.2. Biodistribution and blood clearance

The direct radiolabeling of the aptamer pool and the library allowed radiolabel yields higher than 90%. The effectiveness of this process for labeling the SA20, SA23 and SA34 aptamers has already been demonstrated in a previous study in which the aptamers were successfully labeled with ^{99m}Tc and the radiolabeling stability in saline solution, plasma and cysteine excess was demonstrated (Santos et al., 2015).

The biodistribution was performed at 3 h after radiotracer administration (Fig. 1). The uptake of radioactivity in the right thigh of group 1 mice (infected with *S. aureus* and inoculated with ^{99m}Tc-aptamers) was statistically higher ($p < 0.05$) compared to the control groups (2 and 3). The group 1 showed a high target/non-target ratio of 2.7 ± 0.40, whereas group 2 (infected with *S. aureus* and inoculated with the ^{99m}Tc-library) exhibited a target/non-target ratio of 1.5 ± 0.1. This ratio for the group 3 (non-infected animals inoculated with ^{99m}Tc-aptamers) was 1.0 ± 0.1. The target/non-target ratio found for the group 1 was statistically higher than those observed in the control groups. These results demonstrated the radiotracer usefulness for identification of *S. aureus* infection foci.

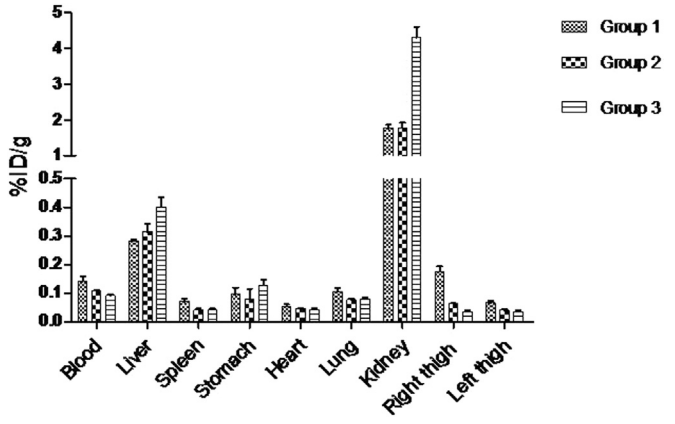

Fig. 1. Biodistribution profiles. The pool of aptamers was labeled with ^{99m}Tc and injected into the tail vein. The mice were euthanized at 3 h post-injection, tissue samples were dissected and their activities were measured in a gamma counter. Group 1 - animals infected with *S. aureus* and inoculated with ^{99m}Tc-aptamers. Group 2 - animals infected with *S. aureus* and inoculated with the ^{99m}Tc-library. Group 3 – Non-infected animals that received the ^{99m}Tc-aptamers.

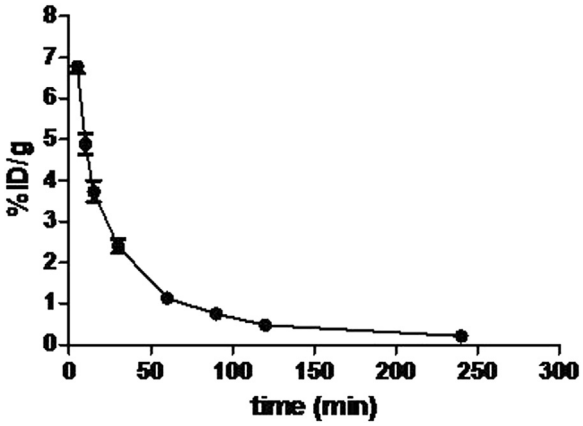

Fig. 2. ^{99m}Tc-aptamers clearance from Swiss mice blood. The ^{99m}Tc-aptamers were administrated through the tail vein. Blood samples (20 μL) were collected at 5, 10, 15, 30, 60, 90, 120, and 240 min after administration. The results were expressed as percentage of injected activity per gram (%ID/g). The distribution half-life was 4.5 min and elimination half-life was 28.4 min.

The biodistribution profile for all groups showed increased uptake in the kidneys indicating a main renal excretion. The uptake in the kidneys was significantly higher in the healthy mice (group 3) than in *S. aureus* infected animals. This finding was probably related to the infection process that may affect the renal function after reaching the bloodstream. Due to chelating agents were not used for the labeling process, the biodistribution profile seems to reflect only the aptamer properties (small, negatively charged and hydrophilic), being not altered by additional molecules.

The clearance of ^{99m}Tc-aptamers from Swiss mice blood is shown in the Fig. 2. The distribution half-life was 4.5 min and elimination half-life was 28.4 min. The ^{99m}Tc-aptamers circulate quickly and they were rapidly cleared from the blood, as reported for other aptamers (Gijs et al., 2016). However, this elimination half-life was higher than expected in view of the aptamers hydrophilic nature and their molecular weight below the molecular cutoff of the renal glomerulus (30–50 kDa). This result was probably due the aptamers binding to plasma proteins, since it delays glomerular filtration and the urinary excretion of oligonucleotides (Younes et al., 2002). However, this elimination half-life prevents very fast aptamers clearance while allowing high target to background contrast in a relatively short time. A too fast renal excretion is disadvantageous for imaging as the radiopharmaceutical will not be able to exert its intended function.

3.3. Scintigraphic imaging

The scintigraphic image profiles obtained after radiotracer administration for all groups showed a high uptake in the bladder (Fig. 3) confirming the urinary tract as the main route of radiotracer elimination. For radiopharmaceuticals elimination, the renal route is preferred over the hepatobiliary clearance pathway, since hepatobiliary clearance is necessary accompanied by a relatively slow gastrointestinal transit. No accumulation of radioactivity was observed in the thyroid or stomach, indicating acceptable levels of radiochemical impurities such as TcO_4^-.

The mice of group 1 showed a visible uptake in the infected right thigh foci at 1 h and 3 h (Fig. 3A), while visible differences were not observed between right and left thighs of the control animals of groups 2 (Fig. 3B) and 3 (Fig. 3C), ratifying the biodistribution results. The target/non-target ratios determined by ROI analysis of images in the group 1 were 4.6 ± 0.7 at 1 h and 4.5 ± 0.6 at 3 h. For group 2, the

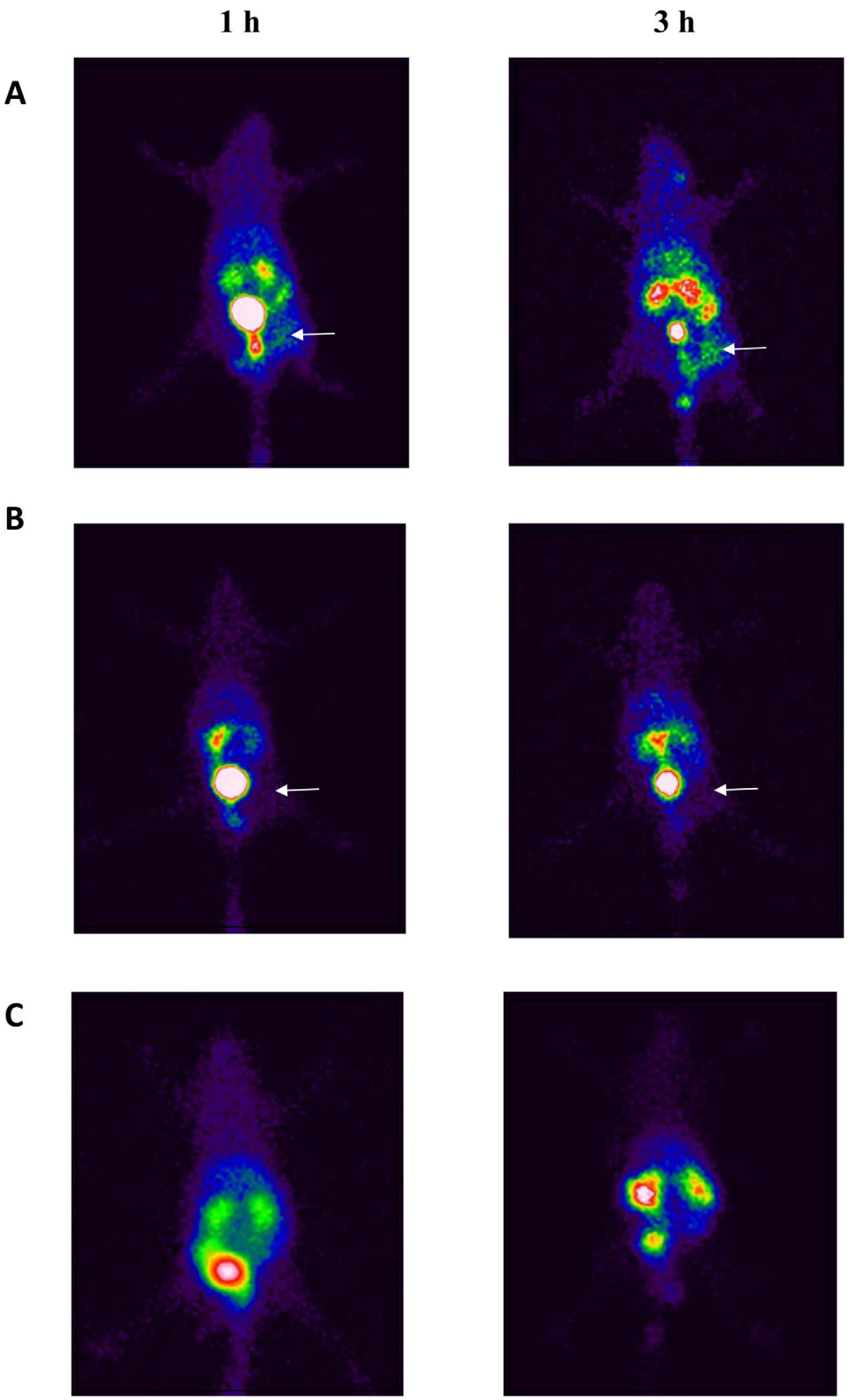

Fig. 3. Scintigraphic images. The figures shown representative images of each mice group. The arrows indicate the infectious foci. **A:** Group 1 (animals infected with *S. aureus* and inoculated with ^{99m}Tc-aptamers). **B:** Group 2 (animals infected with *S. aureus* and inoculated with the ^{99m}Tc-library). **C:** Group 3 (non-infected animals that received the ^{99m}Tc-aptamers).

ratios were 1.6 ± 0.3 and 1.6 ± 0.5, and for group 3, the values were 1.2 ± 0.2 and 0.95 ± 0.2, at the same times (Fig. 4).

Two experimental control groups were used in this study: groups 2 and 3. In the group 2, the mice were infected with *S. aureus* and inoculated with the ^{99m}Tc-library. The ^{99m}Tc-library consists of oligonucleotides with random sequences presenting similar size of the *S. aureus* aptamers but without specificity for the microbial targets. The radiolabeled library acts as blood flow marker and non-specific uptake indicator. The value of 1.6 for the target/non-target ratio verified for ^{99m}Tc-library, at 1 h and 3 h, would be a consequence of the increased capillary permeability and vasodilatation caused by the inflammation process that accompanies infection. In the group 3, were used non-infected animals (which received saline in the right thigh) that were inoculated with the ^{99m}Tc-aptamers. The target/non-target ratios of 1.2

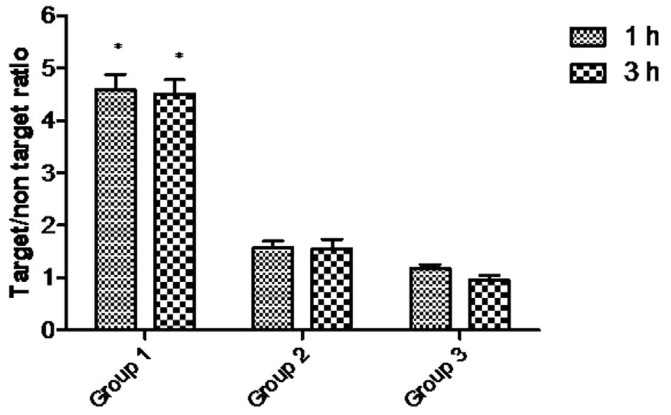

Fig. 4. Target/non-target ratios determined by ROI. The ratios of the count in the target/to non-target ROI were calculated using the total counts. Group 1 - animals infected with *S. aureus* and inoculated with ^{99m}Tc-aptamers. Group 2 - animals infected with *S. aureus* and inoculated with the ^{99m}Tc-library. Group 3 – Non-infected animals that received the ^{99m}Tc-aptamers. The symbol (*) indicates significant difference between the groups ($p < 0.05$).

and 0.95 at 1 h and 3 h, respectively, were compatible with absence of vascular alterations associated to inflammation in the animals of this group.

The radiotracer was constituted of three different *S. aureus* aptamers. The combined use of these aptamers has an additive effect on the *S. aureus* recognition compared to using only a single aptamer (Cao et al., 2009), since these aptamers are not addressed to the same target on the bacterial cell surface. This approach helps to circumvent potential difficulties related to antigenic variations of bacterial cells in the course of the infection, avoiding false negative results.

Current imaging modalities to diagnose infections in nuclear medicine, such as positron emission tomography (PET) and single-photon emission computed tomography (SPECT) are unable to distinguish bacterial infection from other infections, or from sterile inflammation (Love and Palestro, 2004). PET imaging of infections using ^{18}F-fluorodeoxy-glucose (FDG) is of low specificity since all tissues with a high glucose uptake, such heart, brain, sterile inflammation, malignancies and wound healing, show increased FDG uptake (Love et al., 2005). Leukocyte scintigraphy allows to some extent the distinction between inflammation and infection by comparing images at different acquisition times. However, the procedure is very laborious, since it involves the drawing of blood form the patient, harvesting and radiolabeling of leukocytes, and re-administrating of the labeled leukocytes to the patient. In addition, leukocyte scintigraphy is not able to identify the microorganism causing the infection (Glaudemans et al., 2013). ^{67}Ga-citrate is one of the most used radiopharmaceuticals for imaging of infections. However, it has a very low specificity. ^{67}Ga-citrate binds in ionic form to circulating transferrin as an analog of iron. Increased blow flow and increased vascular membrane permeability result in increased delivery and accumulation of transferrin-bounded ^{67}Ga in infected areas but also in areas of aseptic inflammation (Love and Palestro, 2004). Another extensively described approach is the imaging of infection with radiolabeled human polyclonal immunoglobulin (Nijhof et al., 1997), but again the procedure is of low specificity and inflammation often results in a false-positive signal. An emerging area of research involves the use of radiolabeled antibiotics. Most current knowledge in this field concerns ^{99m}Tc-ciprofloxacin. Although the sensitivity of this radiotracer seems promising, its specificity is relatively low (Britton et al., 2002).^{18}F-labeled ciprofloxacin did not allow for bacteria-specific imaging in humans. The signal was not retained in infected tissue and vanished at similar elimination half time as healthy tissue, suggesting that the radioactive signal was related to increased blood flow and vascular permeability in local infection (Langer et al., 2004). Radiolabeled antimicrobial peptides are emerging as an interesting alternative for infection diagnosis. Antimicrobial peptides are an important component of the innate immune system that provides protection against microbial attacks. Ten successful clinical studies have been reported on specific imaging of infection using the radiolabeled peptide ubiquicidin (Ostovar et al., 2013). Despite presenting high specificity for infection, this radiotracer is also not able to identify the microorganism that causes the infection.

The rationale to try aptamers as radiopharmaceuticals for infection diagnosis is that they can bind specifically to microorganisms and might be able to distinguish infection from aseptic inflammation and to identify the type of pathogen causing the infection. Aptamer–based-radiopharmaceuticals have been developed for imaging and tested for preclinical applications. The majority of them have been radiolabeled with ^{99m}Tc for SPECT imaging of cancer-related targets (Hwang et al., 2010; Hicke et al., 2006; Boisgard et al., 2009; Da Pieve et al., 2009; Wu et al., 2014; Varmira et al., 2014). Radiolabeled aptamers for non-cancer diseases imaging have also been reported as for inflammation (Charlton et al., 1997) and thrombus-imaging (Dougan et al., 2003).

The use of radiolabeled aptamers for infection diagnosis is a new approach and only two articles on this subject has been published to date (De Sousa Lacerda et al., 2017; Santos et al., 2015). In the study Santos et al. (2015) an *ex vivo* biodistribution study was performed using the SA20, SA23 and SA34 *S. aureus* radiolabeled aptamers and it was possible to distinguish a *S. aureus* infection from a *Candida albicans* infection and from a sterile inflammation. These results encourage us to explore obtaining scintigraphic images using these aptamers. The results of the present study demonstrated that imaging of *S. aureus* infected areas (group 1) was possible by using the ^{99m}Tc-aptamers and high target/non-target ratios (4.6 ± 0.7 at 1 h and 4.5 ± 0.6 at 3 h) were obtained, confirming the previous *ex vivo* studies. These findings indorse the radiolabeled aptamers potential for bacterial infection imaging by scintigraphy, opening a new possibility of using for these molecules.

4. Conclusion

Scintigraphic images identifying *S. aureus* infectious foci were successfully obtained using the SA20, SA23 and SA34 radiolabeled aptamers. The findings suggested that aptamers could be more extensively studied to develop specific diagnostic radiopharmaceuticals for different infection types.

Acknowledgments

This research was supported by Fundação de Amparo à Pesquisa do Estado de Minas Gerais (FAPEMIG) (TEC-APQ-02247-16).

References

Aerts, A., Impens, N.R., Gijs, M., D'Huyvetter, M., Vanmarcke, H., Ponsard, B., Lahoutte, T., Luxen, A., Baatout, S., 2014. Biological carrier molecules of radiopharmaceuticals for molecular cancer imaging and targeted cancer therapy. Curr. Pharm. Des. 20, 5218–5244.

Boisgard, B.K.R., Jego, B., Siquier, K., Hinnen, F., Dollé, F., Friebe, M., Borkowski, S., Dinkelborg, L., Tavitian, B., 2009. In vivo PET tumor imaging using an [F18] labelled aptamer targeting tenascin-C. J. Nucl. Med. 50, 1594.

Britton, K.E., Wareham, D.W., Das, S.S., Solanki, K.K., Amaral, H., Bhatnagar, A., Katamihardja, A.H.S., Malamitsi, J., Moustafa, H.M., Soroa, V.E., Sundram, F.X., Padhy, A.K., 2002. Imaging bacterial infection with ^{99m}Tc ciprofloxacin (Infecton). J. Clin. Pathol. 55, 817–823.

Cao, X., Li, S., Chen, L., Ding, H., Xu, H., Huang, Y., L, i.J., Liu, N., Cao, W., Zhu, Y., Shen, B., Shao, N., 2009. Combining use of a panel of ssDNA aptamers in the detection of *Staphylococcus aureus*. Nucleic Acid. Res. 37, 4621–4628.

Charlton, J., Sennello, J., Smith, D., 1997. In vivo imaging of inflammation using an aptamer inhibitor of human neutrophil elastase. Chem. Biol. 4, 809–816.

Correa, C.R., Barros, A.L.B., Ferreira, C.A., Goes, A.M., Cardoso, V.N., Andrade, A.S.R., 2014. Aptamers directly radiolabeled with technetium-99m as a potential agent capable of identifying carcinoembryonic antigen (CEA) in tumor cells T84. Bioorg. Med. Chem. Lett. 24, 1998–2001.

Da Pieve, C.D., Perkins, A.C., Missailidis, S., 2009. Anti-MUC1 aptmers: radiolabelling with (99m)Tc and biodistribution in MCF-7 tumor-bearing mice. Nucl. Med. Biol. 36,

703–710.
De Sousa Lacerda, C.M., Ferreira, I.M., Santos, S.R., Barros, A.L.B., Fernandes, S.O., Cardoso, V.N., Andrade, A.S.R., 2017. (1→3)-β-D-glucan aptamers labeled with technetium-99m: biodistribution and imaging in experimental models of bacterial and fungal infection. Nucl. Med. Biol. 46, 19–24.
Dougan, H., Weitz, J.I., Stafford, A.R., Gillespie, K.D., Klement, P., Hobbs, J.B., Lyster, D.M., 2003. Evaluation of DNA aptamers directed to thrombin as potential thrombus imaging agents. Nucl. Med. Biol. 30, 61–72.
Evtugyn, C., Porfireva, A., Stepanova, V., Sitdikov, R., Stoikov, I., Nikolelis, D., Hianik, T., 2014. Electrochemical aptasensor based on polycarboxylicmacrocycle modified with neutral red for aflotoxin B1 detection. Electroanalysis 26, 2100–2109.
Ferro-Flores, G., Ocampo-Garcia, B.E., Melendez-Alafort, L., 2012. Development of specific radiopharmaceuticals for infection imaging by targeting infectious micro-organisms. Curr. Pharm. Des. 18, 1098–1106.
Geiger, A., Burgstalle, r.P., Von Der Eltz, H., Roeder, A., Famulok, M., 1996. RNA aptamers that bind L-arginine with sub-micromolar dissociation constants and high enantioselectivity. Nucleic Acids Res. 24, 1029–1036.
Gijs, M., Aertsa, A., Impens, N., Baatout, S., Luxen, A., 2016. Aptamers as radiopharmaceuticals for nuclear imaging and therapy. Nucl. Med. Biol. 43, 253–271.
Glaudemans, A.W., Galli, F., Pacilio, M., Signore, A., 2013. Leukocyte and bacteria imaging in prosthetic joint infection. Eur. Cell. Mater. 25, 61–77.
Henry, S.P., Johnson, M., Zanardi, T.A., Fey, R., Auyeung, D., Lappin, P.B., Levin, A.A., 2012. Renal uptake and tolerability of a 2′-O-methoxethyl modified antisense oligonucleotide (ISIS 113715) in monkey. Toxicology 301, 13–20.
Hicke, B.J., Stenphens, A.W., Gould, T., Chang, Y.F., Lynott, C.K., Heil, J., Borkowski, S., Hilger, C.S., Cook, G., Warren, S., Schmidt, P.G., 2006. Tumor targeting by an aptamer. J. Nucl. Med. 47, 668–678.
Hwang, D.W., Ko, H.Y., Lee, J.H., Kang, H., Ryu, S.H., Song, I.C., Lee, D.S., Kim, S., 2010. A nucleolin-target multimodal nanoparticle imaging probe for traking cancer cells using an aptamer. J. Nucl. Med. 51, 98–105.
Langer, O., Brunner, M., Zeitlinger, M., Zielger, S., Müller, U., Dobrozemsky, G., Lackner, E., Joukhadar, C., Mitterhauser, M., Wadsak, W., Minar, E., Dudczak, R., Kletter, K., Müller, M., 2004. In vivo and in vivo evaluation of [^{18}F]ciprofloxacin for the imaging of bacterial infections with PET. Eur. J. Nucl. Med. Mol. Imaging 32, 143–150.
Love, C., Palestro, C.J., 2004. Radionuclide imaging of infection. J. Nucl. Med. Technol. 32, 47–57.
Love, C., Tomas, M.B., Tronco, G.G., Palestro, C.J., 2005. FDG PET of infection and inflammation. Radiographics 25, 1357–1368.
Missailidis, S., Perkins, A., 2007. Aptamers as novel radiopharmaceuticals: their applications and future prospects in diagnosis and therapy. Cancer Biother. Radio. 22, 453–468.
Nijhof, N.W., Oyen, W.J., Van Kampen, A., Claessens, R.A., Van Der Meer, J.W., Corstens, F.H., 1997. Evaluation of infections of the locomotor system with indium-111- labeled human IgG scintigraphy. J. Nucl. Med. 38, 1300–1305.
Ostovar, A., Assadi, M., Vahdat, K., Nabipour, I., Javadi, H., Eftekhari, M., Assadi, M., 2013. A pooled analysis of diagnostic value of ^{99m}Tc-ubiquicidin (UBI) scintigraphy in detection of an infectious process. Clin. Nucl. Med. 38, 413–416.
Robert, S., Chambers, S., 2005. Diagnosis and management of *Staphylococcus aureus* infections of the skin and soft tissue. Intern. Med. J. 35, 97S–105S.
Santos, S.R., Corrêa, C.R., De Barros, A.L.B., Serakides, R., Fernandes, S.O., Cardoso, V.N., Andrade, A.S.R., 2015. Identification of *Staphylococcus aureus* infection by aptamers directly radiolabeled with technetium-99 m. Nucl. Med. Biol. 42, 292–298.
Tuerk, C., Gold, L., 1990. Systematic evolution of ligands by exponential enrichment: RNA ligands to bacteriophage T4 DNA polymerase. Science 249, 505–510.
Varmira, K., Hosseinimehr, S.J., Noaparast, Z., Abedi, S.M., 2014. Animproved radiolabelled RNA aptamer molecule for HER2 imaging in cancer. J. Drug. Target 22, 116–122.
Wu, X., Liang, H., Tan, Y., Yuan, C., Li, S., Li, X., Li, G., Shi, Y., Zhang, X., 2014. Cell-SELEX aptamer for highly specific radionuclide molecular imaging og gioblastoma in vivo. PLoS One 9, e90752.
You, K.M., Lee, S.H., Lee, B., 2003. Aptamers as functional nucleic acids: in vitro selection and biotechnological applications. Biotechnol. Bioprocess Eng. 8, 64–75.
Younes, C.K., Boisgard, R., Tavitian, B., 2002. Labelled oligonucleotides as radiopharmaceuticals: pitfalls, problems and perspectives. Curr. Pharm. Des. 6, 1451–1466.